Electronic supplementary materials *Mendeleev Commun.*, 2026, **36**, 82–84

Lithium and potassium batteries using promising organic electrode material based on hexaazatrinaphthylene

Guzaliya R. Baymuratova, Igor K. Yakushchenko, Galiya Z. Tulibaeva, Sergey G. Vasil'ev, Pavel A. Troshin, Alexander F. Shestakov and Olga V. Yarmolenko

Table of Contents

Experimental section

Materials and methods

All reagents and solvents were purchased from Sigma-Aldrich and used as received. Elemental analysis was performed on a Vario MICRO cube CHNS/O elemental analyzer (Elementar GmbH). FTIR spectra were recorded on a Perkin Elmer Spectrum BX 100 spectrometer. Melting points were measured using a BOETHIUS PHMK 05 instrument. SEM images of PTDA samples (both as-prepared powder and cathode surface) were obtained using a ZEISS LEO SUPRA 25 scanning autoemission electron microscope. NMR experiments were performed on a Bruker Avance III spectrometer working at 400.2 MHz for ^{1}H and 100.6 MHz for ^{13}C. ^{1}H-^{13}C cross-polarization (CP) experiments were recorded using 3 ms contact time under proton decoupling and magic angle spinning (MAS) at 12 kHz.

Method of synthesis

To 40 mL of glacial acetic acid, 1.38 g (5 mmol) of 1,2,3,4-phenazinetetrone hydrate (1:2) and 1.07 g (5 mmol) of [1,1'-biphenyl]-3,3',4,4'-tetramine were sequentially added under continuous stirring. The reaction mixture was initially heated to 60–70 °C and maintained at this temperature for 7 hours, followed by further heating to 118 °C for an additional 7 hours, resulting in a total reaction time of 14 hours. During the synthesis, a finely dispersed yellow-brown precipitate formed. The precipitate was filtered and thoroughly washed with 20 mL of glacial acetic acid and 20 mL of water. The product was then transferred to 100 mL of methanol, and the resulting suspension was stirred at 45–50 °C for 24 hours. Subsequently, the precipitate was transferred to 100 mL of tetrahydrofuran and stirred for another 24 hours at room temperature. The solid was filtered and washed sequentially with acetone (30 mL) and hexane (30 mL). Finally, the product was dried under reduced pressure over phosphorus pentoxide, yielding 1.93 g (5 mmol, calculated for one HATN unit) of the target product as a finely dispersed powder, with a yield of 98%. The resulting poly-HATN exhibited high thermal stability, showing no melting or color change up to at least 360 °C.

Identification of poly-HATN

Elemental analysis, found (%): C 66.06; H 3.70; N 19.26; O 11,00. Calculated for $C_{24}N_6H_{10}(H_2O)_3$ (%): C 66.39; H 4.07; N 18.92; O 10.62.

^{1}H solid state NMR (400.2 MHz, MAS 12kHz) δ: 5.6 (br s, 4H), **Figure S1.**

^{13}C NMR (100.6 MHz, CP MAS 12 kHz) δ: 130.1 (br s, 10C), 142.0 (br s, 14C), **Figure S2.**

FTIR (ν/cm^{-1}): 3416, 3227 (C-H), 1614 (asym C=N-), 1487 (C=C), 1356 (C-N), 1183, 1134, 1080 (C-C), 824, 760 (out plane C-C ring deformation). **Figure S3.**

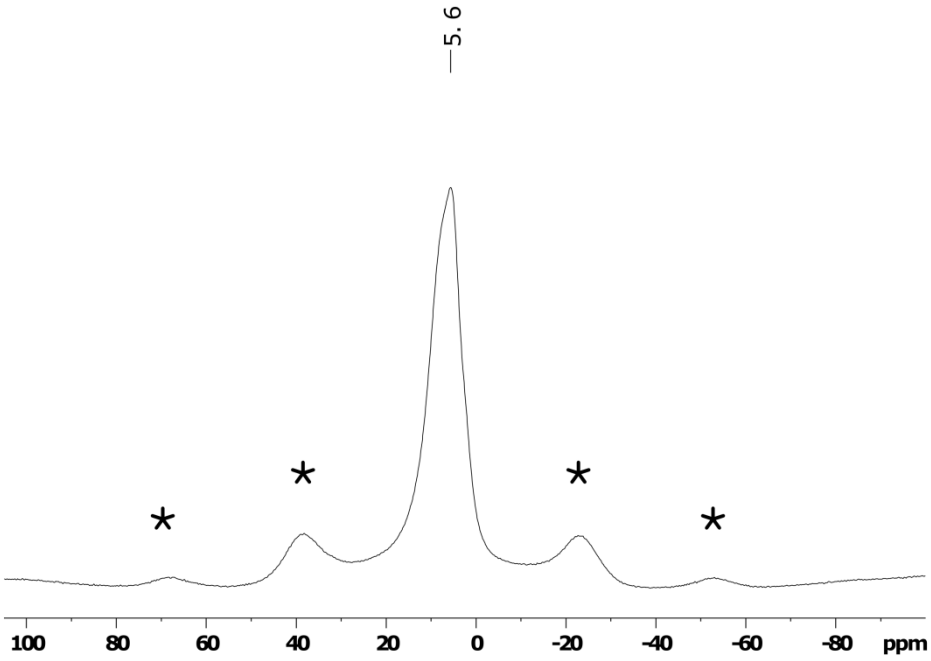

Figure S1 ^{1}H NMR spectrum of poly-HATN (peaks marked with asterisks are MAS spinning sidebands).

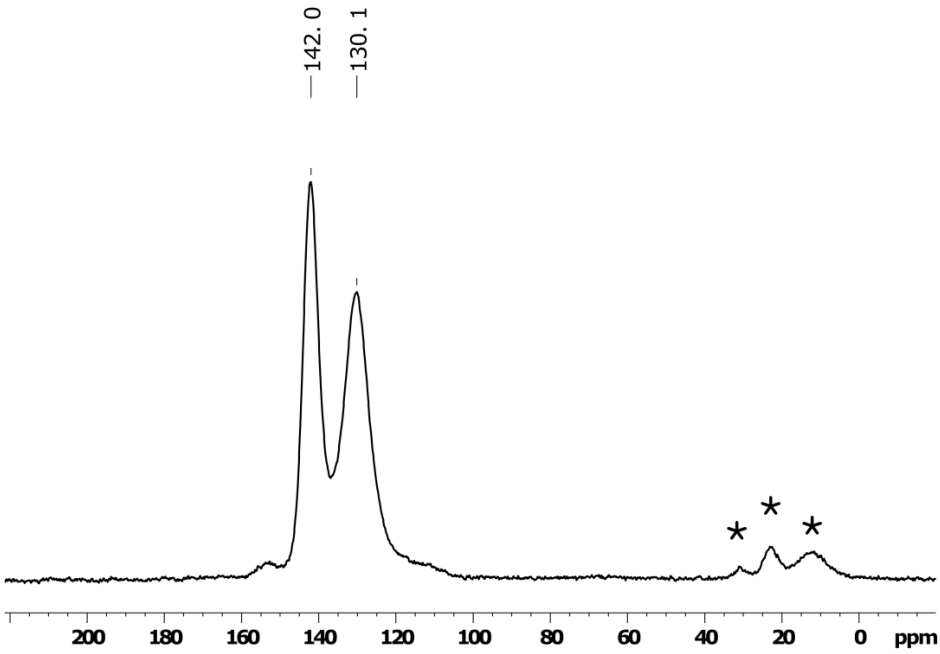

Figure S2 ^{13}C NMR spectrum of poly-HATN (peaks marked with asterisks are MAS spinning sidebands).

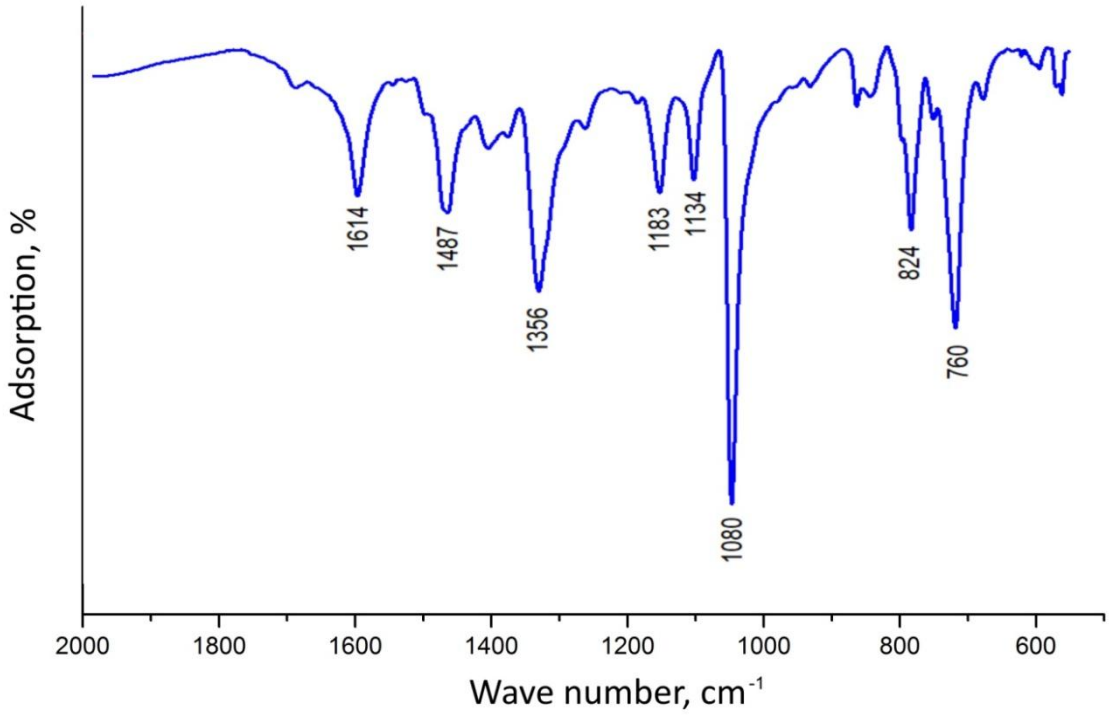

Figure S3 FTIR spectrum of the poly-HATN.

(*a*)

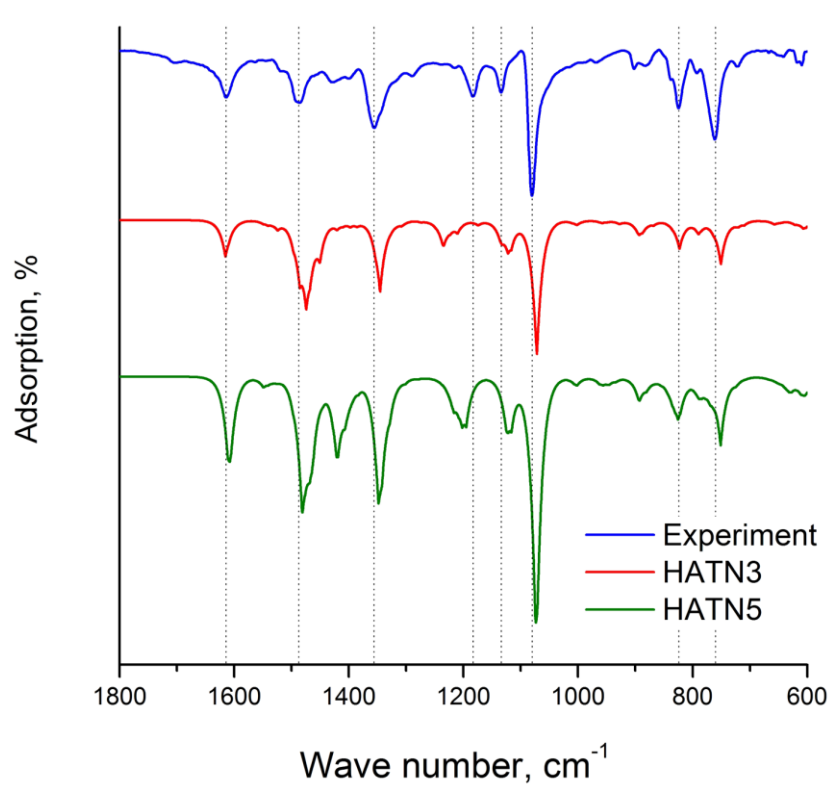

(*b*)

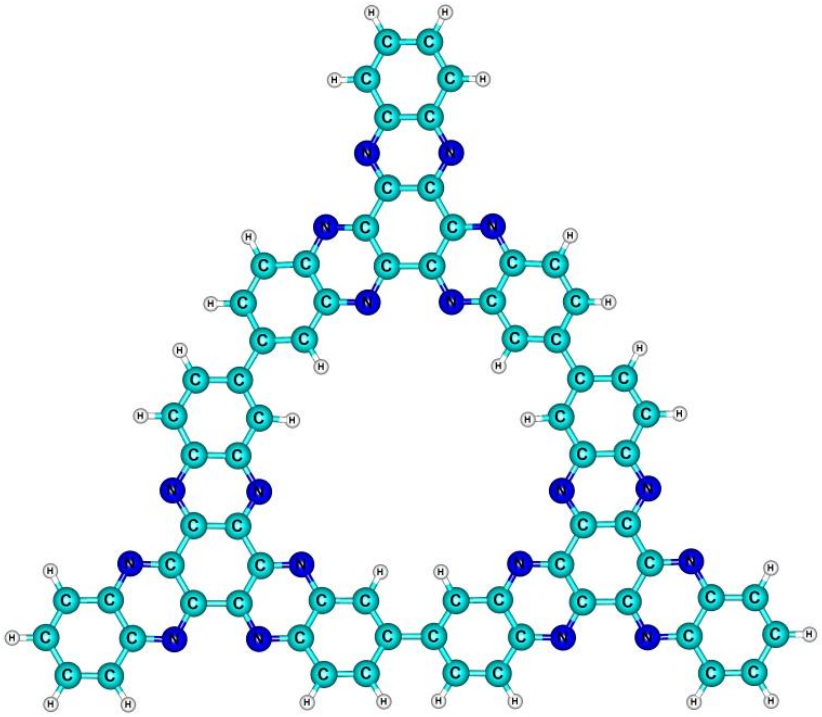

(*c*)

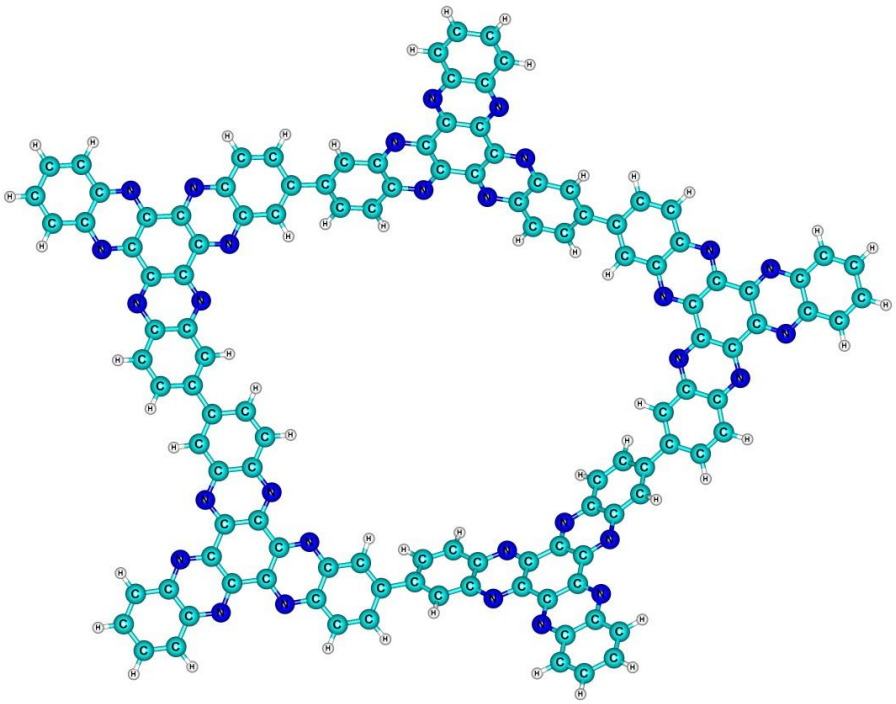

Figure S4 The calculated FTIR spectrum of the poly-HATN with 3 units of HATN (a) and five units of HATN (c) and the experimental FTIR spectrum (a); models of the poly-HATN3 (b) and the poly-HATN5 (c).

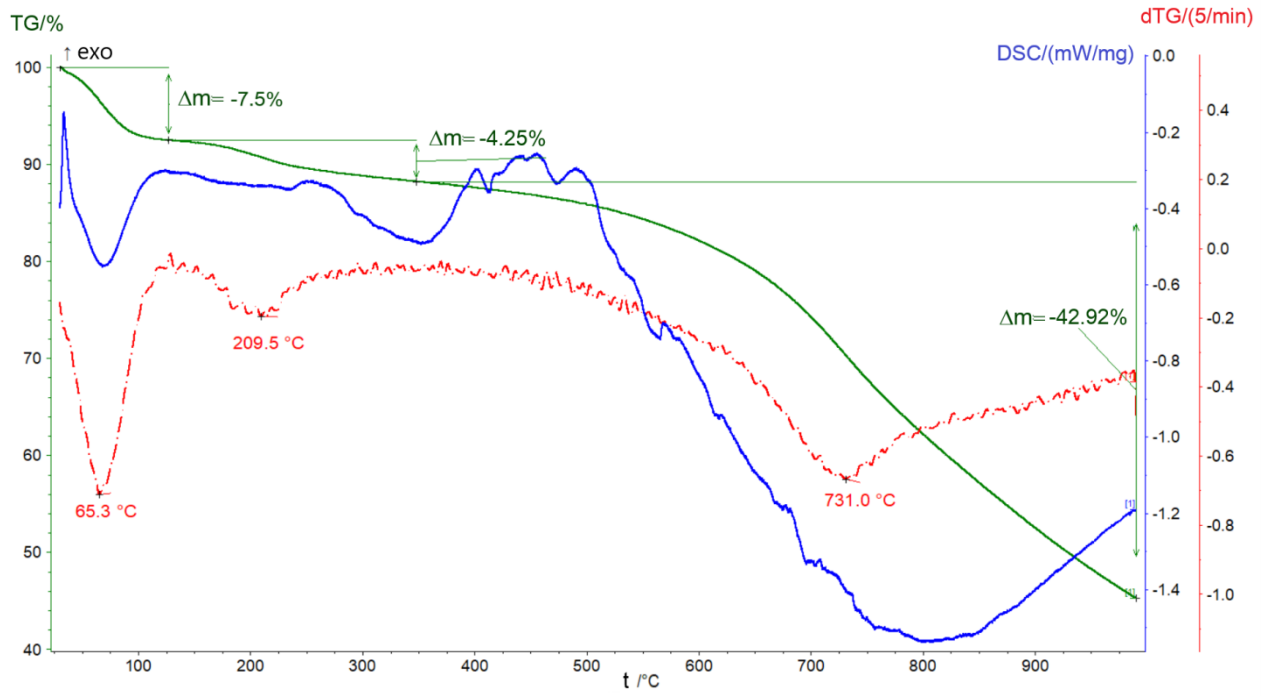

Figure S5 TG and DSC diagrams of the poly-HATN ranging from room temperature to 1000 °C.

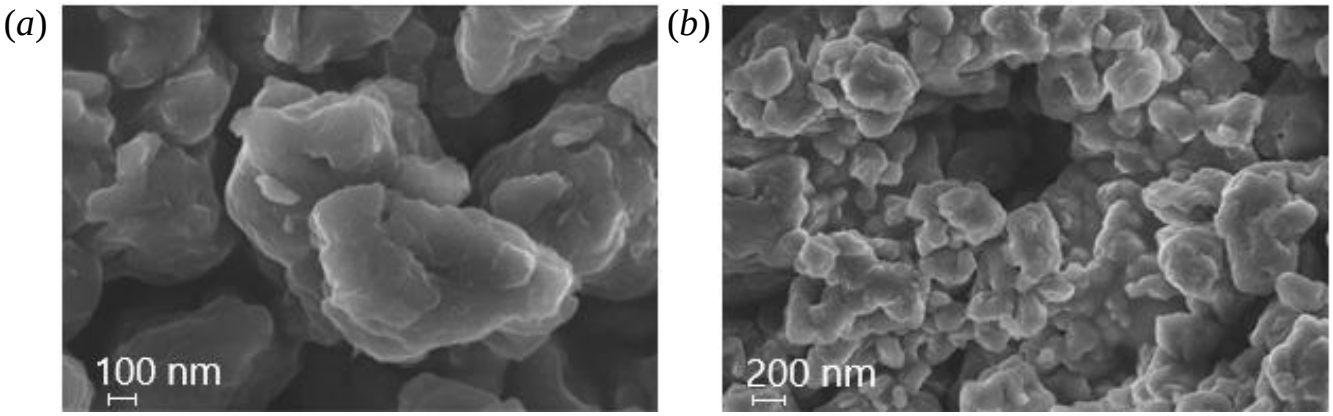

Figure S6 SEM images of the initial poly-HATN powder at a scale of 100 nm (a) and 200 nm (b).

(*a*)

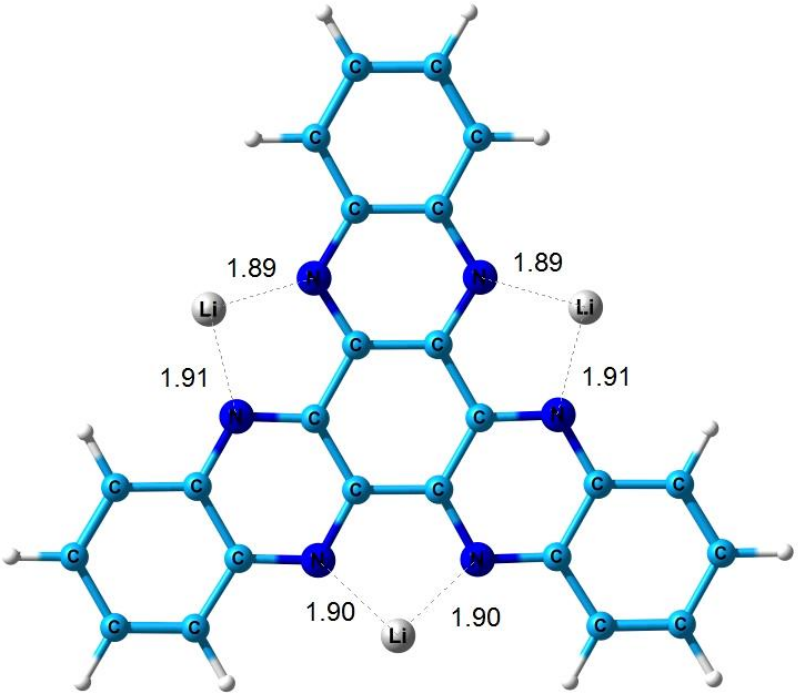

(*b*)

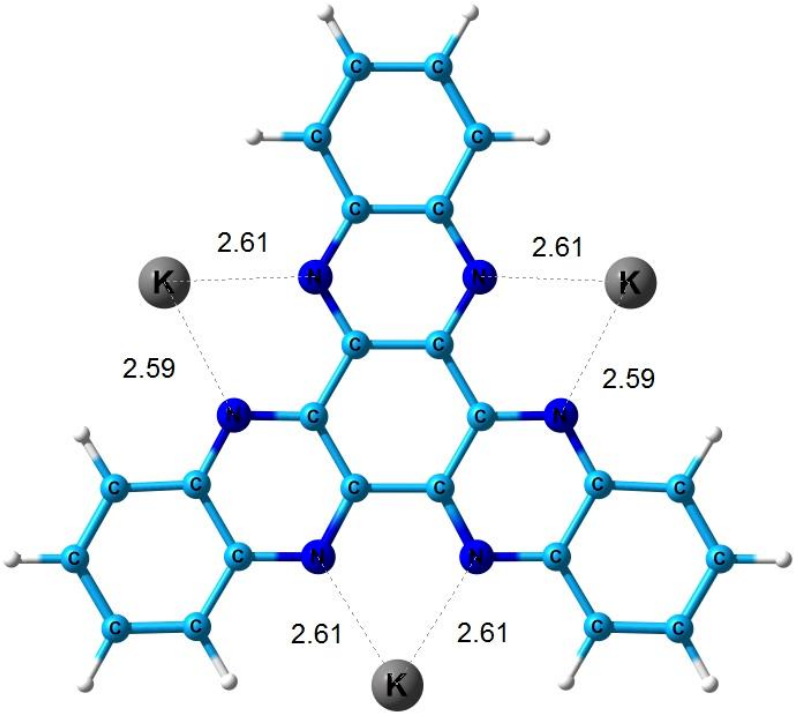

(*c*)

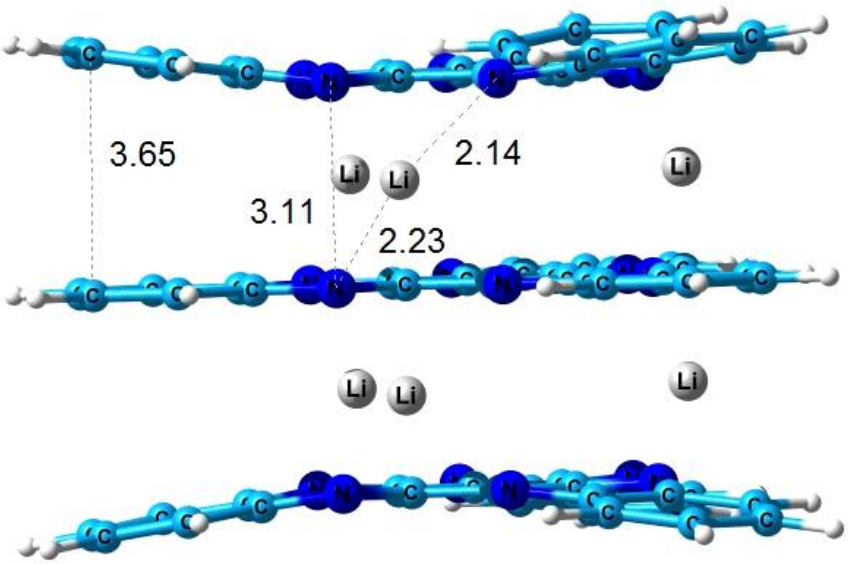

(*d*)

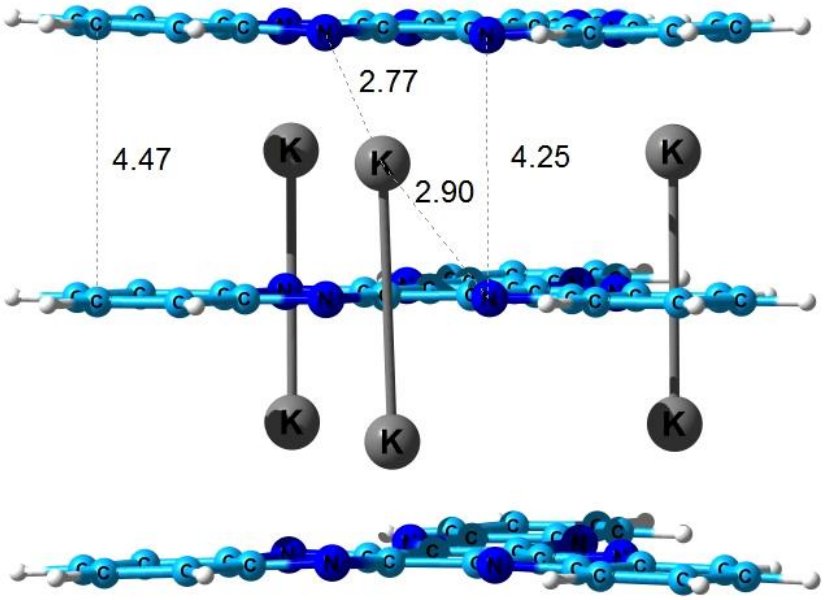

Figure S7 Quantum-chemical modeling of metallation of HATN with 3 atoms of Li (a), with 3 atoms of K (b), complexes of 3 HATN with 6 atoms of Li (c), with 6 atoms of K (d).

(*a*)

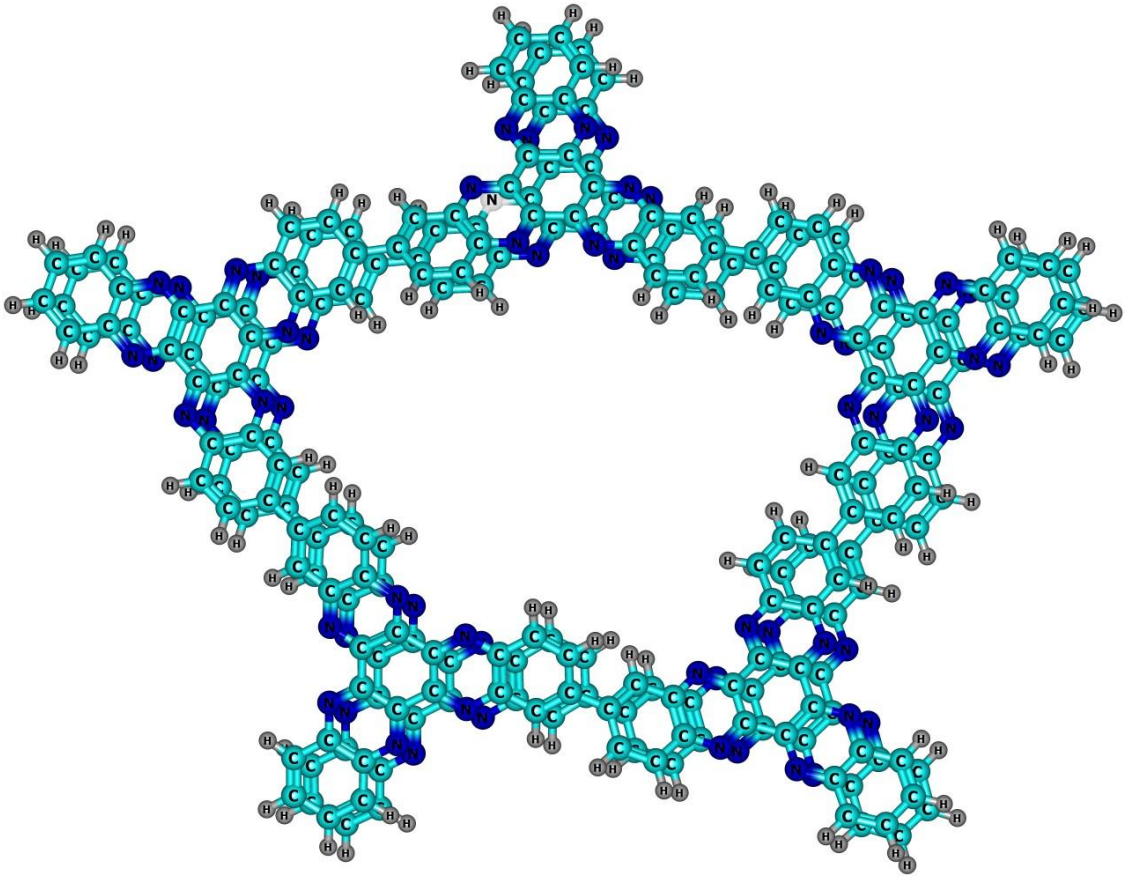

(*b*)

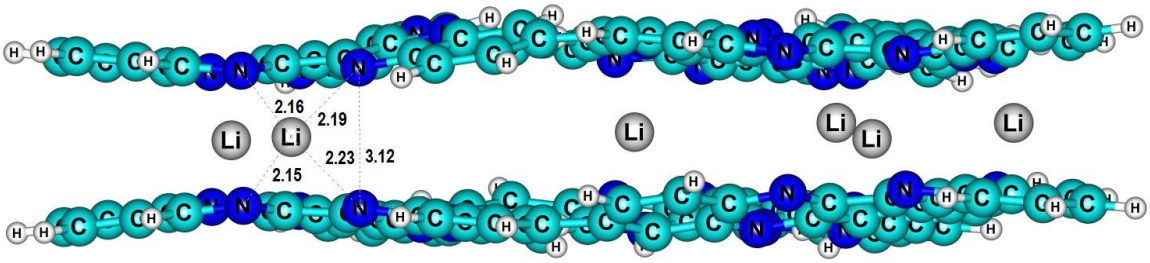

(*c*)

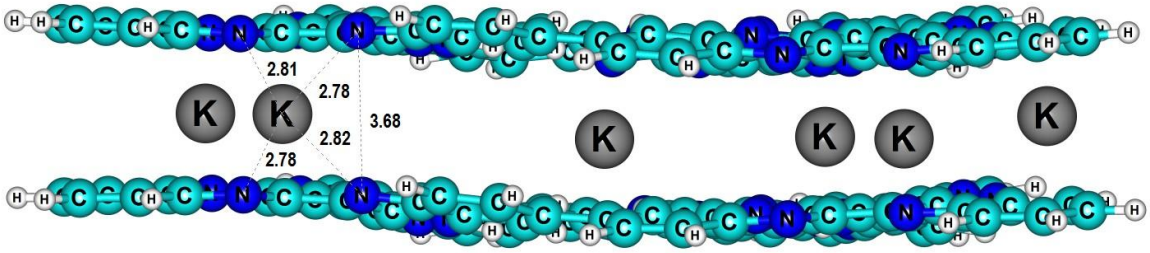

Figure S8 Quantum-chemical modeling of dimer poly-HATN5 (a), metalation of the dimer poly-HATN3 with 6 Li (b) and with 6 K (c).

Electrochemical experiments

Li-Battery Fabrication

The electrochemical performance of poly-HATN was evaluated in the CR2032 coin-type lithium/potassium batteries. The cathode composition comprising of poly-HATN (45 wt%), conductive carbon black (50 wt%, Timical Super C65), and PVDF polymer binder (5 wt%, Kynarflex HSV 900, Arkema France) was dispersed in *N*-methylpyrrolidone (NMP, 99%, Aldrich) to obtain ~12% suspension, which was homogenized mechanically (Light Duty Isolab homogenizer). Cathode slurry was applied onto the current collector (20 μm thick graphitized Al-foil, MTI Corp., USA) using tape coating (Gelon Lib. coater). The resulting films were annealed at 150 °C, pressed on rollers and dried again for 5 hours at a temperature of 120˚C to remove the NMP solvent.

The organic cathode (d = 1.6 cm, active weight of 0.3 mg), polypropylene separator (Celgard 2325, 25 μm) and lithium anode (d = 1.6 cm) were assembled in coin-type lithium batteries using 1 M LiTFSI solution in dimethoxyethane (0.025 ml) as electrolyte.

The organic cathode (d = 1.6 cm, active weight of 0.3 mg), 3 layers of fiberglass separator and potassium anode (d = 1.6 cm) were assembled in coin-type potassium batteries using 1 M KPF_6 solution in dimethoxyethane (0.075–0.1 ml) as electrolyte. The cells were assembled inside MBraun argon glove box.

Li-Battery Testing

Cyclic voltammograms in Li//poly-HATN and K//poly-HATN cells were recorded on a P-40X potentiostat (Elins, Russia) at a sweep rate of 1 mV s^{-1}.

The electrochemical characteristics of the cells were evaluated using a BTS-5V10mA battery analyzer (Neware Technology Ltd., China) cycling at different current values in the range of 1.0–3.5 V.

The value of the charge/discharge current (C) was calculated from the theoretical value of the specific capacitance (C_{theor}) considering the mass of the active layer on the electrode.

$$C/n = (C_{theor} * m_{act})/n \text{ (mAh)} \quad (1)$$

$$C_{theor}(\text{HATN})\ (3e) = 209 \text{ mAh } g^{-1} \quad (2)$$

$$C_{theor}(\text{HATN})\ (6e) = 418 \text{ mAh } g^{-1} \quad (3)$$

Table S1 Potential values of the maxima on the cathodic (E_C) and anodic (E_A) branches of the CV for Li//poly-HATN cells.

Redox transition	Peak potential, V	Cycle number				
		1	2	3	4	5
No.1	E_A	2.85	2.7	2.62	2.56	2.53
	E_C	2.1	2.2	2.24	2.29	2.32
	$\Delta(E_A\text{-}E_C)$	0.75	0.50	0.38	0.27	0.22
No.2	E_A	1.73	1.71	1.65	1.61	1.60
	E_C	-	-	-	1.56	1.56
	$\Delta(E_A\text{-}E_C)$	-	-	-	0.5	0.4

Table S2 Potential values of the maxima on the cathodic (E_C) and anodic (E_A) branches of the CV for K//poly-HATN cells

Redox transition	Peak potential, V	Cycle number				
		1	2	3	4	5
No.1	E_A	2.48/2.33	2.5/2.31			
	E_C	2.27/-	2.4/2.25			
	$\Delta(E_A\text{-}E_C)$	0.21/-	0.1/0.06			
No.2	E_A	2.02	1.95			
	E_C	1.67/-	1.84/1.67			
	$\Delta(E_A\text{-}E_C)$	0.35/-	0.11/0.28			
No.3	E_A	1.25	1.26			
	E_C	1.15	1.16			
	$\Delta(E_A\text{-}E_C)$	0.1	0.1			